

Worm algorithm for the $O(2N)$ Gross-Neveu model

Vidushi Maillart*

*Albert Einstein Center for Fundamental Physics, Institute for Theoretical Physics,
Sidlerstrasse 5, CH-3012 Bern, Switzerland*

*Institute for Theoretical Physics, University of Regensburg, 93040 Regensburg, Germany
E-mail: vidushi.maillart@itp.unibe.ch*

Urs Wenger

*Albert Einstein Center for Fundamental Physics, Institute for Theoretical Physics,
Sidlerstrasse 5, CH-3012 Bern, Switzerland
E-mail: wenger@itp.unibe.ch*

We study the lattice $O(2N)$ Gross-Neveu model with Wilson fermions in the fermion loop formulation. Employing a worm algorithm for an open fermionic string, we simulate fluctuating topological boundary conditions and use them to tune the system to the critical point. We show how the worm algorithm can be extended to sample correlation functions of bound states involving an arbitrary number of Majorana fermions and present first results.

*Speaker.

1. Introduction

It is well known that fermionic degrees of freedom are difficult to simulate on the lattice due to their Grassmannian nature. The fermion matrix determinant, obtained after integrating out the fermion fields, remains the major bottleneck of Monte-Carlo simulations, since it is highly non-local and connects all the degrees of freedom. Each Monte-Carlo update step changes the fermion matrix and requires a new calculation of the determinant. On the other hand, if an algorithm can update the determinant by a local procedure, then a significant gain in efficiency might be achievable. However, simulations of fermions usually suffer from critical slowing down when the fermion correlation length diverges, i.e. when the fermions become massless, and it is by no means obvious whether a local algorithm can be constructed to circumvent this problem.

An interesting attempt to deal with the problems related to simulating fermions on the lattice has recently been suggested in [1, 2] in the context of the $O(2N)$ Gross-Neveu (GN) model. It is based on reformulating the model in terms of closed fermion loops [3, 4, 5]. Introducing an open fermionic string, an algorithm can be devised for which critical slowing is essentially absent. It follows the spirit of Prokof'ev and Svistunov's worm algorithm [6] and makes use of the fact that a global update of the closed fermion loops can be obtained by locally updating the open fermionic string. The open string corresponds to the insertion of a Majorana fermion pair and directly samples the two-point correlation function. In this way the configurations are updated on all length scales up to the correlation length, and this eventually guarantees the absence of critical slowing down. Moreover, the algorithm also allows simulations directly in the massless limit [1, 2] and provides direct access to the critical point via ratios of partition functions [7].

The algorithm has been successfully applied to simulate free fermions in two dimensions, but it has proven equally successfull also in its application to strongly interacting fermions, e.g. in the Schwinger model in the strong coupling limit [1, 2] and in supersymmetric quantum mechanics [8]. Here we report on the application of the worm algorithm to another two-dimensional system of interacting fermions - the $O(2N)$ Gross-Neveu model. We demonstrate how a simple modification of the worm algorithm can be used to measure the fermion bound state spectrum and we present preliminary results for $N = 1$, in which case the GN model corresponds to the Thirring model.

2. Fermion loop formulation of the Gross Neveu model

We consider the two-dimensional $O(2N)$ -symmetric GN model [9] described by the Lagrangian

$$\mathcal{L} = \sum_{i=1}^N \bar{\psi}_i (\gamma_\mu \partial_\mu + m) \psi_i - \frac{g^2}{2} \left(\sum_{i=1}^N \bar{\psi}_i \psi_i \right)^2. \quad (2.1)$$

This is a relativistic quantum field theory of N self-interacting Dirac fermion fields. For $N = 1$ the $O(2)$ GN model is equivalent to the massive Thirring model as $(\bar{\psi} \psi)^2 = \frac{1}{4} (\bar{\psi} \gamma_\mu \psi) (\bar{\psi} \gamma_\mu \psi)$. It has a pseudoscalar bosonic fermion-antifermion bound state [10] and is especially interesting due to its equivalence to the sine-Gordon model [11], in which the boson is the fundamental particle and the fermion emerges as a soliton solution.

To make the model amenable for the fermion loop algorithm in [1], we decompose the complex Dirac fermion fields ψ_j and $\bar{\psi}_j$ into real Majorana fields ξ_{2j} and ξ_{2j+1} according to $\psi_j =$

$(\xi_{2j} + i\xi_{2j+1})/\sqrt{2}$ and $\bar{\psi}_j = (\bar{\xi}_{2j} - i\bar{\xi}_{2j+1})\sqrt{2}$. The Lagrangian density can then be written as

$$\mathcal{L} = \frac{1}{2} \sum_{i=1}^{2N} \bar{\xi}_i (\gamma_\mu \partial_\mu + m) \xi_i - \frac{g^2}{8} \left(\sum_{i=1}^2 \bar{\xi}_i \xi_i \right)^2. \quad (2.2)$$

Note that the $O(2N)$ symmetry is now obvious, as (2.2) is invariant under rotations of the Majorana fields in flavour space. Discretising the action with Wilson fermions gives

$$S = \frac{1}{2} \sum_x \sum_{i=1}^{2N} \varphi \bar{\xi}_i(x) \xi_i(x) - \frac{g^2}{8} \sum_x \left(\sum_{i=1}^{2N} \bar{\xi}_i(x) \xi_i(x) \right)^2 - \sum_{i=1}^{2N} \sum_{x,\mu} (\bar{\xi}_i(x) P(\mu) \xi_i(x + \hat{\mu})), \quad (2.3)$$

where $\varphi = (2+m)$ and $P(\pm\mu) = \frac{1}{2}(1 \mp \gamma_\mu)$. When expanding the Boltzmann factor in the partition function to all orders, terms quadratic or higher order in each field component vanish due to the nilpotency of the Grassmann fields. Restricting now to $N = 1$ for simplicity and keeping only non-trivial terms, the partition function can be written as

$$\begin{aligned} Z = & \int \mathcal{D}\xi \prod_x \left(1 - \frac{\varphi}{2} \left(\sum_{i=1}^2 \bar{\xi}_i(x) \xi_i(x) \right) + \frac{(\varphi^2 + g^2)}{4} \bar{\xi}_1(x) \xi_1(x) \bar{\xi}_2(x) \xi_2(x) \right) \\ & \times \prod_{x,\mu} \prod_{i=1}^2 \left(1 + \bar{\xi}_i(x) P(\hat{\mu}) \xi_i(x + \hat{\mu}) \right) \end{aligned} \quad (2.4)$$

The integration measure is saturated site by site by combinations $\bar{\xi}_i \xi_i$, and it is straightforward to identify the non-vanishing contributions to the partition function. They are characterised by the fact that for a particular Majorana flavour either two adjacent hopping terms and no monomer terms, or one of the monomer terms, but no hopping terms are present at a given site. This results in the constraint that for each flavour only closed, non-intersecting fermion loops survive the Grassmann integration. Furthermore, the loops are non-backtracking due to the orthogonality of the projectors, viz. $P(+\mu)P(-\mu) = 0$. Thus, the partition function is a sum over all possible combinations of two different species of loops (corresponding to the two Majorana flavours). The generalisation to an arbitrary number of N Dirac fields is straightforward – the number of species of loops involved is simply equal to $2N$, the number of Majorana fermions.

3. Worm algorithm for Majorana fermions

In order to generate configurations of closed loops we employ a variant of the algorithm of Prokof'ev and Svistunov [6]. Here we explain the main ideas of the open fermionic string (“worm”) algorithm in a few schematic steps and point out the modifications we have introduced to increase efficiency. Further details can be found in [6, 1].

A peculiar feature of the worm algorithm is that the fermion correlation function is measured during the update procedure. This is due to the fact that the insertion of the open fermionic string, which is used to update the loop configuration, corresponds to the insertion of a pair of Majorana fermions $\xi_i(x)\bar{\xi}_i(y)$ of flavour i at positions x and y , respectively. In the path integral formalism this is equivalent to the correlation function

$$G_i(x,y) = \langle \xi_i(x) \bar{\xi}_i(y) \rangle = \frac{1}{Z} \int \mathcal{D}\xi \xi_i(x) \bar{\xi}_i(y) e^{-S}. \quad (3.1)$$

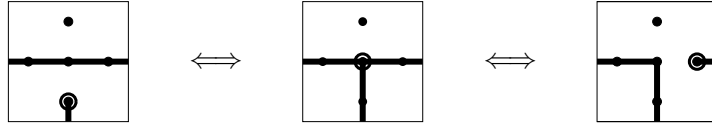


Figure 1: Update moves for the break-up/reconnect step. Note that the configuration in the middle has no physical interpretation and hence gives no contribution to the correlation function.

The algorithm now proceeds by locally updating the ends of the open string using a simple Metropolis procedure according to the weights of the corresponding two-point function. The main steps are as follows:

- *Relocation step:* Given a closed loop configuration, choose a fermion flavour i and a lattice site x at random and place the head ξ_i and the tail $\bar{\xi}_i$ of the worm on this site with a probability given by the weight ratio of the loop configurations before and after the step. If accepted, it gives a contribution to $G_i(x, x)$ unless a loop of species i passes through x in the original closed loop configuration, in which case the new configuration has no physical interpretation and gives no contribution to $G_i(x, x)$.
- *Move step:* Choose a direction μ at random, and move the head of the worm to site $y = x + \hat{\mu}$. Add or delete a fermion bond between x and $x + \hat{\mu}$ depending on whether the bond is empty or occupied. The resulting configuration gives a contribution to $G_i(x, x + \mu)$.
- *Break-up/reconnect step:* In case the new site $x + \hat{\mu}$ is already occupied by a fermion loop of flavour i , we still allow the move, although the corresponding configuration (cf. middle plot in figure 1) is forbidden by the Pauli exclusion principle. Consequently, it does not contribute to the correlation function, but induces transitions between allowed configurations as indicated in the figure.
- *Removal step:* Once the head of the worm reaches its starting position, i.e. head and tail meet again at site x , we may propose to remove head and tail. If accepted, we have a closed loop configuration contributing to the partition function.

We emphasise that the break-up/reconnect step is crucial for the algorithm to work efficiently, since it allows the loops to be opened and restructured. Especially close to the critical point, where loops proliferate, this step gives the worm much more freedom to update the configurations.

4. Topological and fermionic boundary conditions

On a finite lattice with a periodic torus geometry, fermion loops can wind around the lattice and the loop configurations can hence be categorised into different homotopy classes depending on the number of loop windings. For each Majorana fermion ξ_i a two dimensional vector $\vec{l}_i = (l_x, l_t)_i$ is assigned to each configuration to account for the windings in space and time direction, respectively. The components of \vec{l}_i are either 0 or 1 corresponding to an overall even or odd number of loop windings, respectively, in the corresponding direction. Configurations with different \vec{l}_i contribute to separate partition functions $Z_{\vec{l}_1, \vec{l}_2, \dots}$ with fixed topological boundary conditions (b.c.).

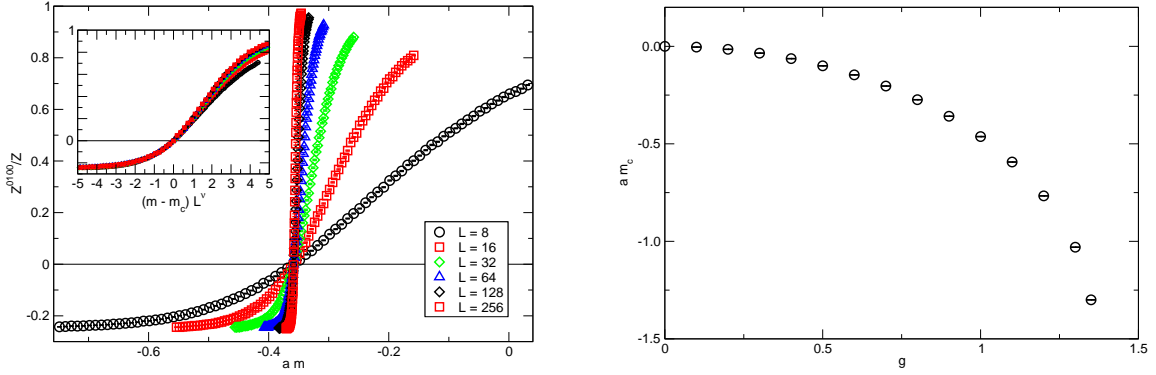


Figure 2: The figure on the left shows the ratio Z^{0100}/Z for the Thirring model at $g = 0.9$ as a function of the bare mass am on square lattices of size $L = 8, 16, 32, 64, 128$ and 256 . The inset shows the finite size scaling. The right plot summarises our results for the critical mass am_c as a function of the coupling g .

Since the open fermion string of the worm algorithm tunnels between the configurations in the various homotopy classes, it samples all the partition functions $Z_{\vec{l}_1, \vec{l}_2, \dots}$. More importantly, the configurations in all homotopy classes are sampled with positive weights relative to each other, i.e. the partition function $Z \equiv \sum_{\vec{l}_1, \vec{l}_2, \dots} Z_{\vec{l}_1, \vec{l}_2, \dots}$ corresponds to one with fluctuating topological b.c., but unspecified fermionic b.c. As a consequence, the b.c. for the fermions can be chosen at the end of the simulation and all possible fermionic b.c. can be studied *a posteriori*.

In order to encode the fermionic b.c. we introduce a two dimensional vector $\vec{\epsilon}_i$ in analogy to \vec{l}_i . The components of $\vec{\epsilon}_i$ are 0 or 1, and correspond to periodic or anti-periodic b.c., respectively. The partition function $Z^{\vec{\epsilon}_1, \vec{\epsilon}_2, \dots}$ for fixed $\vec{\epsilon}_1, \vec{\epsilon}_2, \dots$ can now be written as a linear combination of the partition functions $Z_{\vec{l}_1, \vec{l}_2, \dots}$, e.g. for $N = 1$,

$$Z^{\vec{\epsilon}_1, \vec{\epsilon}_2} = 4Z_{\vec{0}, \vec{0}} - 2 \sum_{\vec{l}_1} (-1)^{\vec{\epsilon}_1 \cdot \vec{l}_1} Z_{\vec{l}_1, \vec{0}} - 2 \sum_{\vec{l}_2} (-1)^{\vec{\epsilon}_2 \cdot \vec{l}_2} Z_{\vec{0}, \vec{l}_2} + \sum_{\vec{l}_1, \vec{l}_2} (-1)^{(\vec{\epsilon}_1 \cdot \vec{l}_1 + \vec{\epsilon}_2 \cdot \vec{l}_2)} Z_{\vec{l}_1, \vec{l}_2}. \quad (4.1)$$

As shown in [7], choosing periodic b.c. for all fermions in all directions, except antiperiodic in one direction for one single fermion, e.g. $\vec{\epsilon}_1 = (0, 1)$ and $\vec{\epsilon}_{i>1} = (0, 0)$, the corresponding partition function $Z^{0100\dots}$ vanishes at the massless, critical point, i.e. when the bare mass m is equal to the critical mass m_c . Hence, the criterion can be used to determine m_c for various couplings by tuning the bare mass m to the point where $Z^{0100\dots} = 0$.

In figure 2 we show the results of such a determination for the Thirring model. The plot on the left shows the partition function ratio Z^{0100}/Z as a function of the bare mass am for square lattices with $L = 8, \dots, 256$ at the coupling $g = 0.9$. As the lattice size increases the jump from $Z^{0100}/Z \sim 1$ to $Z^{0100}/Z \sim -0.25$ is more and more pronounced, so that the critical point $Z^{0100} = 0$ can be determined very precisely. Since the critical point corresponds to a second order phase transition where the correlation length diverges, one should find a corresponding universal finite size scaling (FSS) behaviour. The inset in the left plot of figure 2 illustrates that this is indeed the case. There we show the partition function ratios as a function of $(m - m_c)L^\nu$, and from the FSS we can determine the critical exponent ν and the critical mass am_c in the thermodynamic limit $L \rightarrow \infty$ to a very high precision with a rather modest computational effort. The right plot in

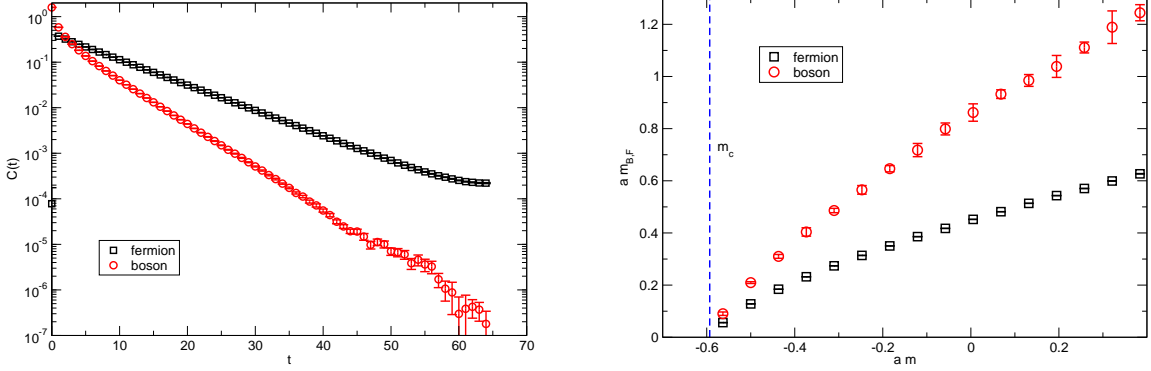


Figure 3: In the left plot the single fermion and bound state correlation functions are plotted. The right plot shows the fermion and boson masses as a function of the bare mass am for the Thirring model at $g = 1.1$.

figure 2 summarises our results for the critical mass in the thermodynamic limit as a function of the coupling g .

5. Bound states of fermions

It can easily be worked out that the correlation function of the pseudoscalar bound state $\bar{\psi} \gamma_5 \psi$ in the Thirring model is given by

$$\langle \mathcal{O}(x) \mathcal{O}(y) \rangle = \langle \bar{\xi}_1(x) \gamma_5 \xi_2(x) \bar{\xi}_1(y) \gamma_5 \xi_2(y) \rangle. \quad (5.1)$$

In the loop formulation, this corresponds to two open fermion strings, one for each Majorana fermion flavour, with common endpoints at positions x and y . In complete analogy to the single fermion update using the fermionic 2-point correlation function, we can update the configurations using the bosonic bound state correlation function in eq.(5.1). In practice, we insert two instances of the bound state wave function $\mathcal{O}(x) = \bar{\xi}_1(x) \gamma_5 \xi_2(x)$ into the system and let them move around by employing again a local Metropolis update. This procedure samples the bound state correlation function, and at the same time updates the loop configuration of both fermion flavours. In order for this to work efficiently, the break-up and reconnection step described in section 3 is the crucial ingredient, since otherwise the algorithm would be restricted to move the bound state wave function only to sites where no fermion loop is present. Obviously, this would become increasingly difficult towards the critical point, where the fermion loops proliferate.

The efficiency of the algorithm is illustrated in figure 3. In the left plot we show the single fermion and the bosonic bound state correlation functions at zero momentum obtained from a simulation of the Thirring model on a $L = 128$ lattice at coupling $g = 1.1$. It is remarkable that in both cases the signal can be followed over several orders of magnitude. Consequently, the corresponding masses can be reliably determined towards the continuum limit. This is illustrated in the right plot of figure 3 where we show the fermion and boson masses versus the bare mass am .

6. Conclusions and outlook

Using Wilson's fermion discretisation, the path integral for the $O(2N)$ Gross-Neveu (GN) model can be described on the lattice in terms of interacting fermion loops. We discussed how the loop system can efficiently be simulated using open fermion strings. Single fermion and bound state correlation functions are measured while updating the system. In addition, the algorithm allows the direct calculation of ratios of partition functions with arbitrary fermion boundary conditions. We have successfully implemented the fermion loop algorithm for $N = 1$, in which case the GN model is equivalent to the Thirring model, and presented first preliminary results for the determination of the critical point from the partition function ratios. Moreover, we also presented first promising results for the single fermion and the bound state masses. Currently we are working on measuring these quantities for the massive Thirring model in the continuum limit at various values of the couplings, in order to compare the results to predictions based on the equivalence of the model to the Sine-Gordon model. The extension of the algorithm to a larger number of fermions is interesting and rather straightforward.

An obvious question to ask is whether and how the idea of updating an open fermionic string can be put to use in the context of gauged fermions or in higher dimensions. Successfull attempts were so far reported only in the strong coupling limit [1, 2, 12], but there are many other interesting and promising extensions [13] using worm-type algorithms, even in connection with pure gauge theories [14].

Acknowledgements

This work has partly been supported by the European Union under grant 238353 (ITN STRONGnet).

References

- [1] U. Wenger, *Phys. Rev.* **D80** (2009) 071503, [[arXiv:0812.3565](#)].
- [2] U. Wenger, *PoS LAT2009* (2009) 022, [[arXiv:0911.4099](#)].
- [3] I. O. Stamatescu, *Phys. Rev.* **D25** (1982) 1130.
- [4] C. Gattringer, *Nucl. Phys.* **B543** (1999) 533–542, [[hep-lat/9811014](#)].
- [5] U. Wolff, *Nucl. Phys.* **B789** (2008) 258–276, [[arXiv:0707.2872](#)].
- [6] N. Prokof'ev and B. Svistunov, *Phys. Rev. Lett.* **87** (2001) 160601.
- [7] O. Bär, W. Rath, and U. Wolff, *Nucl. Phys.* **B822** (2009) 408–423, [[arXiv:0905.4417](#)].
- [8] D. Baumgartner and U. Wenger, *PoS LATTICE2010* (2010) 245, [[arXiv:1104.0213](#)].
- [9] D. J. Gross and A. Neveu, *Phys. Rev.* **D10** (1974) 3235.
- [10] R. F. Dashen, B. Hasslacher, and A. Neveu, *Phys. Rev.* **D11** (1975) 3424.
- [11] S. R. Coleman, *Phys. Rev.* **D11** (1975) 2088.
- [12] S. Chandrasekharan and A. Li, *JHEP* **12** (2010) 021, [[arXiv:1009.2774](#)].
- [13] S. Chandrasekharan, *Phys. Rev.* **D82** (2010) 025007, [[arXiv:0910.5736](#)].
- [14] T. Korzec and U. Wolff, *PoS LATTICE2010* (2010) 029, [[arXiv:1011.1359](#)].